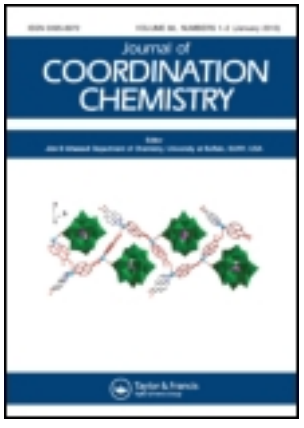

Journal of Coordination Chemistry
Publication details, including instructions for authors and subscription information:
http://www.tandfonline.com/loi/gcoo20

Synthesis, crystal structure and characterization of manganese(III) complex containing a tetradentate Schiff base

Agata Bartyzel[a]
[a] Department of General and Coordination Chemistry, Faculty of Chemistry, Maria Curie-Skłodowska University, Lublin, Poland
Published online: 10 Dec 2013.

To cite this article: Agata Bartyzel (2013) Synthesis, crystal structure and characterization of manganese(III) complex containing a tetradentate Schiff base, Journal of Coordination Chemistry, 66:24, 4292-4303, DOI: 10.1080/00958972.2013.867029

To link to this article: http://dx.doi.org/10.1080/00958972.2013.867029

Journal of Coordination Chemistry, 2013
Vol. 66, No. 24, 4292–4303, http://dx.doi.org/10.1080/00958972.2013.867029

Synthesis, crystal structure and characterization of manganese(III) complex containing a tetradentate Schiff base

AGATA BARTYZEL*

Department of General and Coordination Chemistry, Faculty of Chemistry, Maria Curie-Skłodowska University, Lublin, Poland

(*Received 26 July 2013; accepted 14 November 2013*)

N,N′-bis((2-hydroxyphenyl)(phenyl)methylidene)propane-1,2-diaminato-N,N′,O,O′)-(nitrato-O)-manganese(III) methanol solvate ($[Mn(C_{29}H_{24}N_2O_2)(NO_3)CH_3OH]$) was synthesized and characterized by FTIR, UV–Vis, TG–FTIR, TG/DSC, molar conductivity, magnetic moment measurement and single crystal X-ray analysis. In the structure, the Mn(III) ion adopts a distorted octahedral geometry with two nitrogen and two oxygen atoms from the Schiff base ligand in the equatorial plane, and the nitrate ion and methanol molecule in the axial position. The effects of organic solvents of various polarities on the UV–Vis spectra of the ligand and complex were investigated. The manganese(III) complex is easily dissolved in organic polar aprotic solvents and has moderate solubility in organic polar protic solvents.

Keywords: Tetradenate Schiff base; Manganese(III) complex; Crystal structure; Spectral analysis; Thermal analysis

Introduction

In recent years, interest in the design, synthesis, and coordination chemistry of polydentate chelating ligands capable of forming stable complexes with metal ions has resulted in the study of a large number of new chelating agents. Schiff bases are the ligands which give these opportunities and for this reason have attracted the attention of researchers for many decades. Nowadays, the research field dealing with Schiff base coordination chemistry has expanded enormously. Special attention is paid to the diimine Schiff bases with OH groups in the ortho positions to the amino groups [1–5]. This type of azomethine compound is of interest mainly due to the existence of O–H···N hydrogen bonds and also due to the presence of tautomerism between the keto-amine and enol-imine forms. The tautomerism involves proton transfer from the hydroxylic oxygen to the imino nitrogen atom and this type of Schiff base compound shows solvato-, thermo- and photochromism [6, 7].

In the literature, several Schiff bases have been reported as effective corrosion inhibitors for different metals and alloys in acidic media [8, 9]. Moreover, it is evident that in the azomethine derivatives the C=N linkage is essential for biological activity. Schiff bases have exhibited a broad range of biological activities, including antifungal, antibacterial, antimalarial, antiproliferative, antiinflammatory, antiviral, antioxidant, and antipyretic properties [1–5, 10, 11].

*Emails: adaxe13@wp.pl; agata.bartyzel@poczta.umcs.lublin.pl

The main idea of this work was synthesis and characterization of N,N′-bis((2-hydroxyphenyl)(phenyl)methylidene)propane-1,2-diaminato-N,N′,O,O′)-(nitrato-O)-manganese(III) methanol solvate (**1**), which was obtained during reaction of manganese(II) nitrate with N,N′-bis((2-hydroxyphenyl)(phenyl)methylidene)propane-1,2-diamine in methanol. The complex has been characterised by microanalytical, spectroscopic, molar conductivity, magnetic moment, thermal, and single-crystal X-ray diffraction studies. A similar compound was reported by Ghosh and co-workers [1] and was synthesised by reaction of the manganese(II) chloride and the Schiff base in methanol. Structural study indicates that the complex described by Ghosh and co-workers was composed of discrete five-coordinate Mn(III) units with a distorted square-pyramidal geometry and crystallised in a monoclinic system ($P2_1/n$) [1]. In contrast, reported in this paper, the compound crystallizes in the $P2_1/c$ group and the manganese(III) ion adopts distorted octahedral geometry. The hydrogen bonds between methanol and nitrate molecules, which are coordinated to the metal center, link the molecules in infinite chains parallel to [001].

Experimental

Materials

The 1,2-propanediamine and 2-hydroxybenzophenone used for the preparation of the Schiff base were obtained from the Aldrich Chemical Company. The metal salt $Mn(NO_3)_2{\cdot}4H_2O$ was purchased from Merck. All the organic solvents were purchased from Polish Chemical Reagents (Poland). All solvents and chemicals were reagent grade and were used without further purification.

The N,N′-bis((2-hydroxyphenyl)(phenyl)methylidene)propane-1,2-diamine (scheme 1) was synthesized according to the method described in a previous paper [12] (51.4% yield. Elemental analysis of $C_{29}H_{26}N_2O_2$. Calcd (%): C 80.18; H 5.99; N 6.45. Found (%): C, 79.92; H, 5.99; N, 6.04).

Synthesis (1)

The mixture of stoichiometric amounts of manganese(III) nitrate (0.005 M) and Schiff base (0.005 M) in 20 mL of methanol were put into a 100 mL Teflon vessel. The next reaction mixture was heated up to 50 °C for 20 min and kept for 3.5 h. The content of vessel was stirred during the whole time of synthesis and then cooled. The solution was left for few days until all of the solvent had evaporated. The solid, brown product was washed with cold methanol, dried in air, and later recrystallized from methanol. The single crystal suitable for X-ray analysis was obtained by slow evaporation solvent at 4 °C after a few weeks.

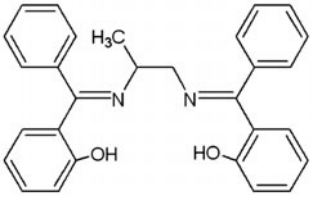

Scheme 1. Schiff base ligand.

Methods and physical measurements

Elemental analysis for C, H, and N was performed using a Perkin–Elmer CHN 2400 analyzer. Magnetic susceptibility measurement was conducted at 295 K using a magnetic susceptibility balance, MSB-MKI (Sherwood Scientific Ltd, Cambridge, UK). The data was corrected for diamagnetic susceptibilities [13, 14]. The effective magnetic moment was calculated from the equation $\mu_{eff} = 2.828(\chi_{cor}T)^{1/2}$. The molar conductivities were measured at 25 °C with a PHY-WE 13701.93 conductivity meter. The infrared spectra were acquired using a Thermo Scientific Nicolet 6700 FTIR with a Smart iTR diamond ATR accessory. Data was collected between 4000 cm^{-1} and 600 cm^{-1}, with a resolution of 4 cm^{-1} for 16 scans. The UV–Vis spectra were acquired on a Genesys 10s spectrophotometer (Thermo Scientific), using 1.0 cm quartz cells.

Single-crystal diffraction data was collected on an Oxford Diffraction Xcalibur CCD diffractometer with graphite-monochromated MoKα radiation (λ = 0.71073Å). The temperature for the experiment was maintained at 100 K with an Oxford Cryosystem N_2 gas-stream cooling device. The programs CrysAlis CCD and CrysAlis Red [15] were used for data collection, cell refinement, and data reduction. A semi-empirical absorption–correction based upon the intensities of equivalent reflections was applied, and the data was corrected for Lorentz and polarization effects. The structure was solved by direct methods using SHELXS97 and refined by the full-matrix least-squares on F^2 using the SHELXL97 [16] (both operating under WinGX [17]). All non-hydrogen atoms were refined with anisotropic displacement parameters. H atom bonded to O atom was located in a difference Fourier map and refined using a riding model. The positions of hydrogen atoms residing on carbon atoms were positioned geometrically and refined applying the riding model[C–H = 0.95–0.98 Å and with $U_{iso}(H) = 1.2$ or $1.5U_{eq}(C)$].

The X-ray diffraction pattern was taken on a HZG–4 (Carl Zeiss-Jena) diffractometer using Ni filtered Cu Kα radiation. The measurement was made within the range 2θ = 5–55.5° with a step equal to 0.05°. The X-rayan program was used for determining position and peak intensities. The TREOR [18] program was used for calculating the unit cell parameters from the collection of data, which had been obtained from the X-rayan program.

Thermal stability and decomposition of the analyzed complex was determined by a Setaram Setsys 16/18 derivatograph, recording TG, DTG, and DSC curves. The sample (7.39 mg) was heated in a ceramic crucible between 30 and 700 °C in flowing air atmosphere with a heating rate of 10 °C min^{-1}. TGA/infrared spectrometry (TG-FTIR) of the title compound was performed using the TGA Q5000 analyzer (TA Instruments) interfaced to the Nicolet 6700 FT-IR spectrophotometer. About 22.36 mg of (**1**) was put in an open ceramic crucible and heated up to 1000 °C in flowing nitrogen atmosphere (heating rate 20 °C min^{-1}).

Results and discussion

The Mn(III) complex was obtained as dark brown yellow crystals, which are stable at room temperature, both in solution and in the solid state. The yield of the purified complex was 64.7%. Purity of the compound was established by elemental analysis and X-ray diffraction patterns. Elemental analysis (Anal. Calcd for $[Mn(C_{29}H_{24}N_2O_2)(NO_3)CH_3OH]$(%): C, 61.91; H, 4.81; N, 7.22. Found(%): C, 61.83; H, 4.77; N, 7.56) showed that obtained manganese(III) complex is pure compound. The data from X-ray powder diffraction analysis confirmed that the analyzed complex represents a single phase. Moreover, during recrystallization significant changes in the crystal structure did not take place. The solution of powder diffraction is also monoclinic, with the parameters a = 18.495(7) Å, b = 9.781(2) Å,

c = 15.878(4) Å, and V = 2719.08 Å^3 (F_{20} = 3.(0.028185, 254) [19]), giving evidence that the unit cell parameters are similar for single crystal and powder data. The room temperature magnetic moment of the studied complex is 5.04 BM. The value is closed to the reported values expected for high-spin complexes of transition metal ions with an octahedral geometry and d^4 configuration, i.e. 4.80–5.00 BM. This value confirms that Mn^{2+} was oxidized to Mn^{3+}. What is more, the value is a slightly different to the spin-only moment (4.90 BM), which indicates some orbital contribution in the magnetic moment [14, 20].

The complex is easily dissolved in organic polar aprotic solvents and has moderate solubility in organic polar protic solvents. The molar conductivity value of a 10^{-3} M L^{-1} solution of (1) determined at 25 °C in THF solvent is almost zero (0.4 Ω^{-1} cm^2 M^{-1}), indicating its non-electrolytic nature in this solvent. The values of the molar conductivity found in remaining solvents (see table 1) indicate uni-univalent (1 : 1) electrolyte behavior. Moreover, it also indicates that the nitrate anion, coordinated to Mn(III), is exchanged by the appropriate solvent molecule in solution [21].

Crystal structure

The molecular structure of the complex is displayed in figure 1. The crystallographic and refinement data for (**1**) are summarized in table 2, selected bond distances and angles are listed in table 3, and hydrogen bond parameters are given in table 4. The complex crystallizes in monoclinic space group $P2_1/c$. In this compound, the Mn ion is in an octahedral environment consisting of O1, O2, N1, and N2 donor atoms (two phenoxo oxygen and two imine nitrogen atoms) from the Schiff base ligand in equatorial positions and two oxygen atoms from the nitrate ion and methanol molecule in axial positions. Within the equatorial plane there is no significant distortion: the Mn–O and Mn–N bond lengths have similar values, 1.864(2) and 1.869(2) Å for Mn–O, 1.991(3) and 1.989(3) Å for Mn–N, and are close to the values reported by Ghosh *et al*. [1]. The equatorial donor atoms O1, O2, N2, and N1 are nearly co-planar, with slight deviation from the mean plane: –0.037, 0.037, –0.053, and 0.053 Å, respectively, and the Mn ion lies on the mean plane. As expected for the Mn(III) ion, the axial Mn–O3 and Mn–O4 distances (2.238(3) and 2.326(2) Å, respectively) are longer than the two Mn–O distances in equatorial sites, due to the Jahn–Teller distortion of the Mn(III) ion. The angles, which are 90° and 180° in a regular octahedral arrangement, range from 84.2(1)° to 96.6(1)° and from 173.8(1)° to 174.9(1)°. Therefore, all data of the above demonstrate that the Mn(III) cation exhibits a distorted octahedral coordination.

The structure is stabilized by hydrogen bonds. The O–H group of methanol is involved in a strong intermolecular hydrogen bond with the nitrate molecule (O3–H3m···O5^{i}, (i) x, $-y + 1/2$, $z + 1/2$) (table 4). This hydrogen bond links the molecules to form infinite chains along the [001] direction (figure 2). It is worth pointing here that the short contacts between O3–O6 and O3–N3 are observed (3.375(4) Å and 3.424(4) Å, and ∠DHA 136.7 and 159.9, respectively). These contacts are short because of the packing that the crystal presents but are not hydrogen bonds and are not responsible for the energetic stability of the packing. However, they affect the crystal packing; the significant disorders in the nitrate ion and methanol molecule are observed [22]. In structure, there are also week intra- and intermolecular C–H···O hydrogen bonds which stabilize the structure (table 4). The C15–H15C group is involved in a three-center bifurcated intramolecular hydrogen bond with two oxygen atoms of nitrate molecule (O4 and O5). The remaining C–H···O interactions are intermolecular and the presence of these hydrogen bonds lead to the formation of a three-dimensional network.

Table 1. Electronic spectra and molar conductivity data.

Solvent	Ligand λ_{max} [nm] ($\varepsilon \times 10^{-4}$ [L M^{-1} cm^{-1}])[a]	Complex λ_{max} [nm] ($\varepsilon \times 10^{-4}$ [L M^{-1} cm^{-1}])[a]	Complex Λ_m [Ω^{-1} cm^2 M^{-1}][b]
H_2O	–[c]	211 (2.85) 236 (4.08) 279 (2.01)^{sh} 307 (1.48)^{sh} 386 (0.60)	–[c]
MeOH : H_2O(1 : 1 v/v)	208 (3.89)^{sh} 260 (1.98) 325 (0.54) 400 (0.31)	206 (5.87)^{sh} 236 (4.29) 280 (2.06)^{sh} 304 (1.52)^{sh} 350 (0.74)^{sh} 394 (0.61)	–[c]
MeOH	229 (2.47) 258 (2.05) 323 (0.72) 399 (0.24)	204 (6.42) 239 (4.28) 282 (2.01)^{sh} 309 (1.48)^{sh} 349 (0.75)^{sh} 399 (0.60)	112.6
EtOH	213 (4.11) 258 (2.08) 323 (0.75) 406 (0.19)	210 (4.92) 240 (4.15) 282 (1.96)^{sh} 311 (1.40)^{sh} 349 (0.73)^{sh} 400 (0.60)	39.0
DMF	268 (1.65) 323 (0.82)	268 (2.16) 283 (1.78)^{sh} 310 (1.21)^{sh} 402 (0.52)	85.5
ACN	211 (4.78) 257 (2.00) 321 (0.80)	213 (3.89) 239 (4.27) 285 (1.94)^{sh} 314 (1.39)^{sh} 351 (0.87)^{sh} 402 (0.59)	75.5
THF	219 (3.90) 259 (2.06) 325 (0.91)	222 (2.72) 246 (3.08) 284 (1.78)^{sh} 312 (1.30)^{sh} 407 (0.49)	0.4

a – concentration 2.5×10^{-5}; b – concentration 1.0×10^{-3}, T = 24 °C; c – not measured,sh – shoulder, MeOH – methanol, EtOH – ethanol, ACN – acetonitryl, DMF – N,N-dimethyloformamide, THF – tetrahydrofurane.

FT-IR analysis

In the solid state, N,N′-bis((2-hydroxyphenyl)(phenyl)methylidene)propane-1,2-diamine exists in enol form [12]. The O–H stretching frequency of the free ligand is expected in the 3500–3300 cm^{-1} region. However, in the o-hydroxy Schiff bases this band is generally moved to lower frequencies (3200–2500 cm^{-1}) due to the presence of a strong intramolecular hydrogen bond O–H···N=C. As the hydrogen bond becomes stronger, this band becomes

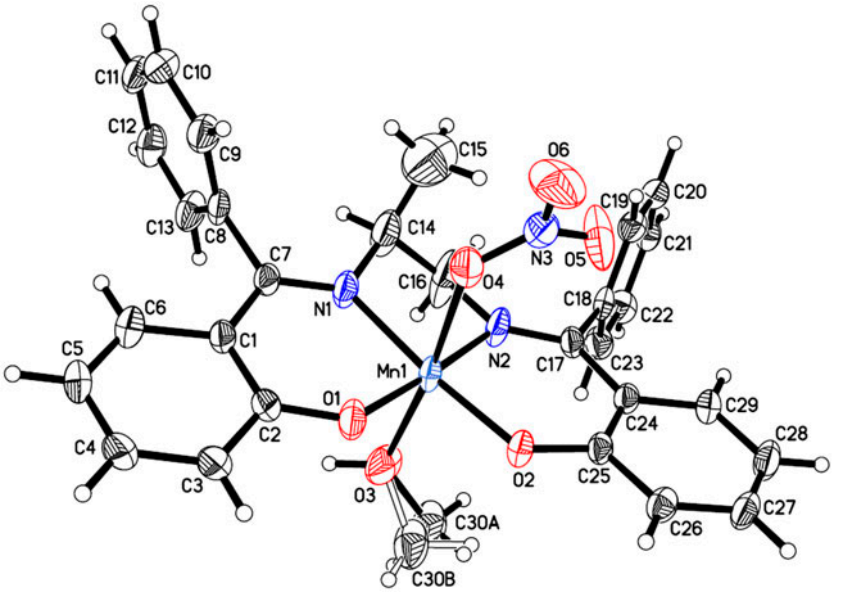

Figure 1. Perspective view of (**1**) with the atom numbering scheme. Displacement ellipsoids are draw at the 50% probability level. The C30 atom of the methanol molecule is disordered, occupying two statistical positions represented by C30A and C30B with site occupancy factors equal to 0.59 and 0.41, respectively.

Table 2. Crystal data and structure refinement for (**1**).

Formula	$[Mn(C_{29}H_{24}N_2O_2)(NO_3)CH_3OH]$
Formula weight	581.49
Temperature (K)	100(2)
Crystal system	Monoclinic
Space group	$P2_1/c$
a(Å)	19.0997(8)
b(Å)	9.9176(4)
c(Å)	15.7546(6)
β(°)	113.833(5)
Volume (Å^3)	2729.8(2)
Z	4
Calculated density (g cm^{-3})	1.415
μ (mm^{-1})	0.533
Absorption correction	Multi-scan
F (000)	1208
Crystal size (mm)	0.15 × 0.15 × 0.10
θ Range (°)	2.49 to 27.48
Index ranges	$-12 \le h \le 24$
	$-11 \le k \le 12$
	$-20 \le l \le 15$
Reflections collected/unique	11186/6239
R_{int}	0.0364
Data/restraints/parameters	6239/0/368
GOF on F^2	0.999
Final R indices [$I > 2\sigma(I)$]	$R_1 = 0.0578$, $wR_2 = 0.1548$
R indices (all data)	$R_1 = 0.0945$, $wR_2 = 0.1674$

Table 3. Selected bond lengths [Å] and angles [°].

Bond lengths (Å)			
N(1)–Mn(1)	1.991(3)	O(2)–Mn(1)	1.869(2)
N(2)–Mn(1)	1.989(3)	O(3)–Mn(1)	2.238(3)
O(1)–Mn(1)	1.864(2)	O(4)–Mn(1)	2.326(2)
Bond angles (°)			
O(1)–Mn(1)–O(2)	93.6(1)	N(2)–Mn(1)–O(3)	87.1(1)
O(1)–Mn(1)–N(2)	174.9(1)	N(1)–Mn(1)–O(3)	91.2(1)
O(2)–Mn(1)–N(2)	90.9(1)	O(1)–Mn(1)–O(4)	85.7(1)
O(1)–Mn(1)–N(1)	91.5(1)	O(2)–Mn(1)–O(4)	93.8(1)
O(2)–Mn(1)–N(1)	174.4(1)	N(2)–Mn(1)–O(4)	96.6(1)
N(2)–Mn(1)–N(1)	84.2(1)	N(1)–Mn(1)–O(4)	84.2(1)
O(1)–Mn(1)–O(3)	90.2(1)	O(3)–Mn(1)–O(4)	173.8(1)
O(2)–Mn(1)–O(3)	91.2(1)		

Table 4. Hydrogen-bond geometry [Å, °].

D–H···A	*d*(D–H)	*d*(H···A)	*d*(D···A)	∠ DHA
O(3)–H(3M)···O(5)$^{(i)}$	0.95	1.76	2.684(3)	163
C(11)–H(11)···O(4)$^{(ii)}$	0.95	2.50	3.319(5)	144
C(13)–H(13)···O(6)$^{(i)}$	0.95	2.53	3.451(5)	163
C(15)–H(15C)···O(4)	0.98	2.55	3.171(6)	121
C(15)–H(15C)···O(5)	0.98	2.54	3.508(7)	171
C(21)–H(21)···O(2)$^{(iii)}$	0.95	2.54	3.232(4)	130

Symmetry codes: (i) $x, -y + 1/2, z + 1/2$; (ii) $-x + 1, y + 1/2, -z + 1/2$; (iii) $x, y + 1, z$.

broader and is sometimes not detected [23–25]. In the spectrum of N,N′-Bis((2-hydroxyphenyl)(phenyl)methylidene)propane-1,2-diamine the ν(O–H) band is not observed, indicating that hydrogen bonds O–H···N are strong. Moreover, the stretching vibration band ν(C=N) occurs at lower frequency at 1604 cm^{-1}, which confirms the strong influence of hydrogen bonds on electron density of the C=N groups. This band in the complex shifts to lower frequency (1596 cm^{-1}) compared to the free ligand, indicating a decrease in the C=N bond order due to the coordinate bond formation between the Mn(III) ion and the imine nitrogen lone pair [2, 26, 27]. The Schiff base ligand also coordinates the Mn(III) ion via deprotonated phenolic oxygen. The phenolic O–H deformation band at 1328 cm^{-1} has not occurred in the spectrum of complexes and also the stretching vibration C–O is shifted to a lower frequency (1240 cm^{-1}) compare to the free ligand (1256 cm^{-1}) [26, 28]. The manganese(III) ion is also coordinated by one molecule of methanol and nitrate ion. The peak characteristic for ν(O–H) vibration is shifted to a lower frequency (3183 cm^{-1}) and adsorption appears as a broad, weak band as a result of reduction of the electron density on the hydroxyl oxygen. Moreover, the stretching vibration C–O band from methanol at 1009 cm^{-1} is observed. In the studied complex, the coordination of the monodentate nitrate ion is nonlinear and symmetry C_s is observed. The bands 1625 and 1330 cm^{-1} are assigned to asymmetric and symmetric stretching ν(NO_2) modes whereas the vibration that occurs at 901 cm^{-1} is probably due to stretching NO vibration [29–32]. The remaining bands characteristic of the NO_3^- ion are listed in table S1 (see online supplemental material at http://dx.doi.org/10.1080/00958972.2013.867029).

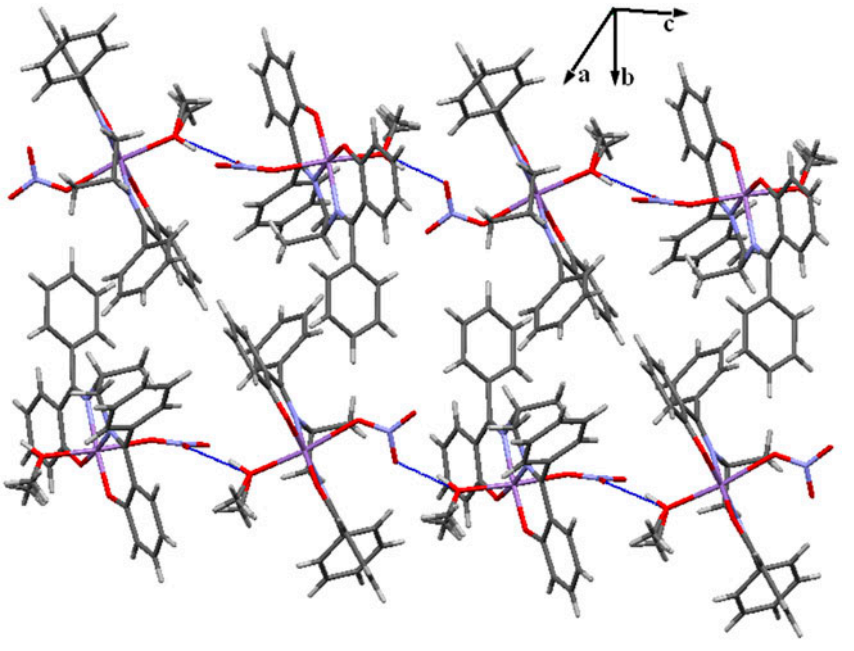

Figure 2. Part of the crystal structure of manganese(III) complex showing strong intermolecular hydrogen bond and formation of 1-D chains along the c-axis.

Electronic absorption spectra

The electronic absorption spectra the data of the title compound and ligand in protic and aprotic solvents are summarized in table 1. As can be seen from the Table, of the UV–Vis spectra of the Schiff base depend on the type of solvent used. The spectrum of the free Schiff base exhibits three or four bands (except the spectrum recorded in the DMF solvent). The two bands which are observed at the range 211–229 nm and 257–268 nm can be assigned to $\pi\rightarrow\pi^*$ transition of the aromatic ring. The next band at 321–325 nm is due to $\pi\rightarrow\pi^*$ transition of the azomethine group. In protic solvent at the range 399–406 nm, a new band is observed and can be attributed to $n\rightarrow\pi^*$ transition of the azomethine group [33, 34]. The appearance of this band in polar protic solvent gives information about enolimine-ketoamine tautomerism of N,N′-bis((2-hydroxyphenyl)(phenyl)methylidene)propane-1,2-diamine. In polar aprotic solvent (DMF, ACN, THF), similar to the solid state [12], the ligand is present predominantly in the enolimine form with a strong intramolecular OH···N=C bond. According to the literature, the new band at 399–406 nm, which appears in polar protic solvents, can be linked with the shift of the tautomeric equilibrium to the ketoamine form [7, 35, 36]. It worth mentioning that the intensity of this band increases with the polarity of used solvents, which can confirm the stabilization of the more polar ketoamine form in more polar solvent. The UV–Vis spectrum of the metal compound contains bands characteristic of the ligand as well as of the Mn(III) ion. The intense absorption bands at about 204–222 and 236–246 nm with two or three shoulder peaks may be assigned to intraligand $\pi\rightarrow\pi^*$ transitions in the complex. Usually, the Mn(III) complex with octahedral geometry gives one charge transfer band around 400 nm and a spin allowed d-d

transition band around 500 nm. In the studied complex, the charge transfer band is observed at 386–407 nm. This band may be attributed to the phenolate $O(p_\pi) \rightarrow Mn(d_{\pi^*})$ ligand-to-metal charge transfer by analogy with related manganese(III) complexes combined with $n \rightarrow \pi^*$ transitions of (C=N) [37, 38]. For (**1**), this band shows a blue shift when the polarity of the solvent is increased. The second band, characteristic of Mn(III) compounds (ca. 500), is not observed on the spectrum of the studied complex due to the low intensity of the d-d transition for used concentration. In more concentrated solutions, this band appears as a shoulder peak ca. 490 nm.

Thermal analysis (TG/DSC and TG/FT-IR)

Thermal analyses of the complex were carried out by the TG/DSC (air) and TG/FTIR (nitrogen) techniques. The thermoanalytical curves TG/DTG and DSC for the complex are presented in figure 3. The Mn(III) complex is stable at room temperature. The first changes in the mass on TG curves (endothermic peak on DSC) occurred above 175 °C (for air) and 105 °C (for nitrogen). The observed mass losses for this step are 7.43% and 7.79%, respectively, for air and nitrogen analysis. The values are similar, indicating that the first stage is probably the same in both cases and is mainly related to the release of methanol. However, the calculated mass lost for the desolvation process is lower (5.50%) than those found on the TG curves, which suggests that an additional process takes place at this step. The FTIR spectra of the evolved gas phase (figure 4, figure S1) confirm that methanol is the main product released during this stage; the characteristic vibration bands are observed in the wavenumber wavenumber ranges 3750–3600, 3150–2750, and 1100–950 cm^{-1}. Moreover, the FTIR spectra obtained during this interval (see figure S1; Supplemental material) show the presence of week bands characteristic of the N_2O (double peak at 2250–2150 cm^{-1}) and CO_2 (2450–2300 cm^{-1} and 750–600 cm^{-1}) [39–41] which indicates that: (i) NO_3^- molecules are partly removed from coordination sphere of Mn(III) ions and (ii) release of CO_2 is probably associated with partial methanol combustion.

Next stage on TG curve recorded in air is observed at the range 250-335 °C and corresponds with a complete removal of NO_3^- from the crystal structure as well as destruction and combustion of part of the ligand. During this stage intermediate, unstable product is formed; the mass loss is 25.23% whereas the calculated weight loss for methanol and nitrate ion is 16.16%. In air atmosphere the final product of decomposition of the complex above 530 °C corresponds to formation of Mn_2O_3 [41, 42] (found and calculated total weight losses are 86.45% and 86.43%, respectively).

In nitrogen atmosphere, the further thermal decomposition of (1) proceeds in three steps and it can be observed from TG curve that the decomposition process was not completed (figure 3). The step between 185 and 250 °C is assigned to a further removal of NO_3^- as well as destruction and combustion part of the ligand. The experimental weight loss of this level is equal 13.96%. This stage is connected with the release of NH_3, N_2O, NO, CO_2, acetamide and methyl isocyanate (figure S2). The major bands for NH_3 are observed in the range 750–1200 cm^{-1} with the characteristic double-peak bands of the maxima at 965 and 931 cm^{-1} [39, 40, 43]. The bands corresponding to NO are recorded at the range 1950–1750 cm^{-1} with a characteristic peak at 1875 cm^{-1} [39]. The bands with maxima which appear between peaks characteristic of CO_2 and N_2O (2311, 2305 and 2294 cm^{-1}) are probably due to methyl isocyanate. The peaks at the range 1800–1700, 1650–1550 and 1450–1200 cm^{-1} correspond to acetamide. The next stage on TG curve is observed at the range

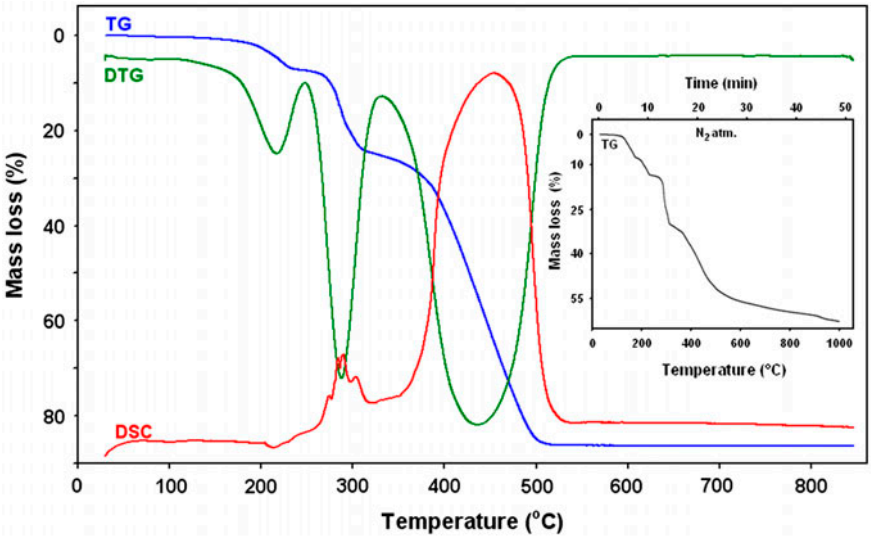

Figure 3. TG, DTG, and DSC curves for the studied ligand in air and the TG curve in nitrogen.

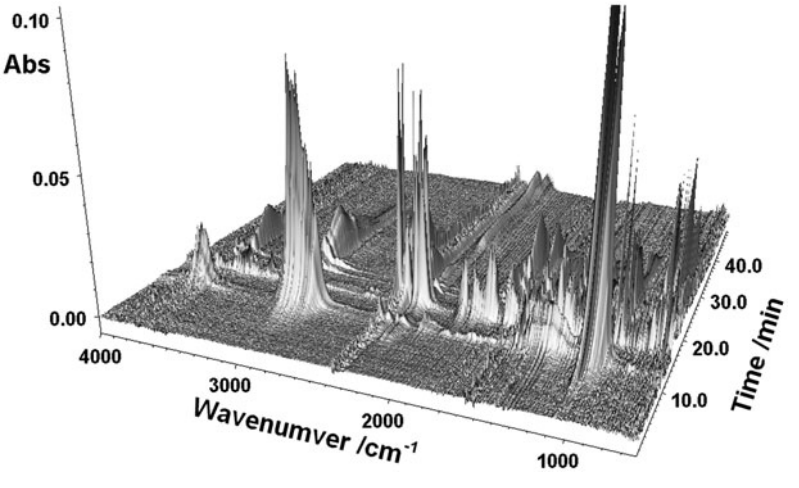

Figure 4. FTIR spectra of gaseous products evolved during the decomposition of the analyzed compound.

280–330 °C with mass loss 31.12%. During this interval the same processes like in previous step are observed i.e. the removal to the remaining of NO_3^- and destruction and combustion next part of the ligand. The gaseous products released during this stage are similar to those that are observed in the previous step with more intense bands associated with the combustion of the Schiff base. Moreover, at higher temperature the week bands characteristic of phenol are also observed. The last stage above 330 °C corresponds to further destruction and combustion of the ligand. At the beginning of this step, the following gases, phenol, benzonitrile, NH_3, CO_2, and methyl isocyanate, were detected in FTIR spectra (figure S3). The bands characteristic for phenol are recorded at the range 3700–3600, 3150–3000,

1650–1100 and 850–650 cm^{-1} [40]. The bands corresponding to benzonitrile occurred at the range 3100–3000, 2275–2200, 1550–1450, and 825–650 cm^{-1}. At a higher temperature (ca. 600 °C), phenol, benzonitrile, and ammonium bands disappeared in the spectra, whereas new peaks characteristic of methane (at the range 3175–2900 cm^{-1} with characteristic maximum at 3016 cm^{-1}) [44] and CO (double peaks at 2275–2050 cm^{-1}) [40, 41] are recorded (see figure S4; Supplemental material).

Conclusion

The Mn(III) complex has been synthesized and characterized by FTIR, UV–Vis, TG-FTIR, TG/DSC, molar conductivity, magnetic moment measurement, and single crystal X-ray analysis. Compared to the synthesis condition reported by Ghosh *et al*. [1], using different substrate (manganese(II) nitrate instead of chloride) and changing the synthesis method, it allowed us to obtain a new six-coordinated metal complex where the Mn(III) ion is coordinated through a N2O2 tetradentate Schiff base, nitrate ion, and methanol molecule. The adjacent mononuclear units are linked by strong hydrogen bonds (O_{MeOH}–H···$O_{nitrate}$) to form a one-dimensional network which is further cross-linked by weak C–H···O interactions and extend into a three-dimensional network. In methanol solution, the nitrate ion coordinated to metal is replaced by molecules of the solvent, in contrast to the chloride ion [1], and the compound behaves as 1 : 1 electrolyte. What is more, the higher value of magnetic moment (5.04 BM) of $[Mn(C_{29}H_{24}N_2O_2)(NO_3)CH_3OH]$ indicates some orbital contribution in the magnetic moment whereas the magnetic moment value reported for $[Mn(C_{29}H_{24}N_2O_2)Cl]$ (4.83 BM [1]) is near to the spin-only moment.

Supplementary material

Crystallographic data have been deposited with the CCDC, 12 Union Road, Cambridge, CB2 1EZ, UK (fax: +44 1223 366033; e-mail: deposit@ccdc.cam.ac.uk or www://www.ccdc.cam.ac.uk) and are available on request, quoting the deposition number CCDC 952312.

References

[1] M. Ghosh, M. Fleck, B. Mahanti, A. Ghosh, G. Pilet, D. Bandyopadhyay. *J. Coord. Chem.*, **65**, 3884 (2012).
[2] R.K. Dubey, P. Baranwal, A.K. Jha. *J. Coord. Chem.*, **65**, 2645 (2012).
[3] Y. Lu, D.-H. Shi, Z.-L. You, X.-S. Zhou, K. Li. *J. Coord. Chem.*, **65**, 339 (2012).
[4] A. Bartyzel, E.M. Cukrowska. *Anal. Chim. Acta*, **707**, 204 (2011).
[5] M. Gowri, C. Jayabalakrishnan, T. Srinivasan, D. Velmurugan. *Mol. Cryst. Liq. Cryst.*, **569**, 151 (2012).
[6] E. Hadjoudis, I.M. Mavridis. *Chem. Soc. Rev.*, **33**, 579 (2004).
[7] V.I. Minkin, A.V. Tsukanov, A.D. Dubonosov, V.A. Bren. *J. Mol. Struct.*, **998**, 179 (2011).
[8] M. Behpour, S.M. Ghoreishi, M. Salavati-Niasari, B. Ebrahimi. *Mater. Chem. Phys.*, **107**, 153 (2008).
[9] M.A. Hegazy. A.M. Hasan, M.M. Emara, M.F. Bakr, A.H. Youssef, *Corros. Sci.*, **65**, 67 (2012).
[10] C.M. da Silva, D.L. da Silva, L.V. Modolo, R.B. Alves, M.A. de Resende, C.V.B. Martins, Â. de Fátima. *J. Adv. Res.*, **2**, 1 (2011).
[11] Z.-Q. Liu, D. Wu. *J. Phys. Org. Chem.*, **22**, 308 (2009).
[12] R.S. Black, D.G. Billing, A. Bartyzel, E.M. Cukrowska. *Acta Cryst.*, **E66**, o1256 (2010).
[13] G.A. Bain, J.F. Berry. *J. Chem. Educ.*, **85**, 532 (2008).
[14] K. Burger. *Coordination chemistry: experimental methods*., Akademia Kiadó, Budapest (1973).
[15] Oxford Diffraction, *Xcalibur CCD System, CrysAlis Software System*, Version 343 1.171, Oxford Diffraction Ltd. (2009).
[16] G.M. Sheldrick. *Acta Crystallogr.*, **A64**, 112 (2008).

[17] L.J. Faruggia. *J. Appl. Crystallogr.*, **32**, 837 (1999).
[18] P.E. Werner. *TREOR, Trial and Error program for Indexing of Unknown Powder 341 Patterns, University of Stockholm, S 106 91*., Stockholm, Sweden (1984).
[19] G.S. Smith, R.I. Snyder. *J. Appl. Cryst.*, **12**, 60 (1979).
[20] D. Moreno, V. Daier, C. Palopoli, J.-P. Tuchagues, S. Signorella. *J. Inorg. Biochem.*, **104**, 496 (2010).
[21] W.J. Geary. *Coord. Chem. Rev.*, **7**, 81 (1971).
[22] J.J. Novoa, F. Mota, E. d'Oria, In: *Hydrogen Bonding-New Insights*, S.J. Grabowski, Chap. 5, pp. 193–244, Springer, Dordrecht (2006).
[23] É. Tozzo, S. Romera, M.P. dos Santos, M. Muraro, R.H.A. de Santos, L.M. Lião, L. Vizotto, E.R. Dockal, *J. Mol. Struct*., **876**, 110 (2008).
[24] H.H. Freedman. *J. Am. Chem. Soc.*, **83**, 2900 (1961).
[25] K. Ueno, A.E. Martell. *J. Phys. Chem.*, **59**, 998 (1955).
[26] B. Cristóvão, B. Miroslaw. *Inorg. Chim. Acta*, **401**, 50 (2013).
[27] M. Rasouli, M. Morshedi, M. Amirnasr, A.M.Z. Slawin, R. Randall. *J. Coord. Chem.*, **66**, 1974 (2013).
[28] R. Takjoo, A. Hashemzadeh, H.A. Rudbari, F. Nicolò. *J. Coord. Chem.*, **66**, 345 (2013).
[29] C.C. Addison, B.M. Gatehouse. *J. Chem. Soc.*, **613**, (1960).
[30] M.R. Rosenthal. The myth of the non-coordinating anion, *J. Chem. Educ.*, **50**, 331 (1973).
[31] V.R. Morris, S.C. Bhatia, J.H. Hall Jr. *J. Phys. Chem.*, **94**, 7414 (1990).
[32] R.P. McLaughlin, B. Bird, P.J. Reid. *Spectrochim. Acta Part A*, **A58**, 2571 (2002).
[33] B. Bosnich. *J. Am. Chem. Soc.*, **90**, 627 (1968).
[34] C.N.R. Rao. *Ultra-Violet and Visible spectroscopy. Chemical application*, Warsaw: PWN (1980).
[35] P. Jeslin Kanaga Inba, B. Annaraj, S. Thalamuthu, M.A. Neelakantan, *Spectrochim. Acta Part A,* **104**, 300 (2013).
[36] N. Galić, Z. Cimerman, V. Tomišić. *Spectrochim. Acta Part A*, **71**, 1274 (2008).
[37] A. Neves, S.M.D. Erthal, I. Vencato, A.S. Ceccato, Y. Mascarenhas, O.R. Nascimento, M. Horner, A.A. Batista. *Inorg. Chem.*, **31**, 4749 (1992).
[38] I.M. Mustafa, M.A. Hapipah, M.A. Abdulla, T.R. Ward. *Polyhedron*, **28**, 3993 (2009).
[39] G. Li, C.A. Jones, V.H. Grassian, S.C. Larsen. *J. Catal.*, **234**, 401 (2005).
[40] A. Dziewulska-Kułaczkowska, A. Bartyzel. *J. Mol. Struct.*, **1033**, 67 (2013).
[41] Z. Rzączyńska, A. Bartyzel, T. Głowiak. *Polyhedron*, **22**, 2595 (2003).
[42] A. Dziewulska-Kułaczkowska. *J. Therm. Anal. Cal.*, **109**, 7 (2012).
[43] Z. Rzączyńska, A. Bartyzel, T. Głowiak. *J. Coord. Chem.*, **56**, 77 (2003).
[44] R. Bassilakis, R.M. Carangelo, M.A. Wójtowicz. *Fuel*, **80**, 1765 (2001).